Journal of Translational Autoimmunity 8 (2024) 100228

Contents lists available at ScienceDirect

Journal of Translational Autoimmunity

journal homepage: www.sciencedirect.com/journal/journal-of-translational-autoimmunity

ANKRD22 aggravates sepsis-induced ARDS and promotes pulmonary M1 macrophage polarization

Shi Zhang [a,b], Yao Liu [c], Xiao-Long Zhang [d], Yun Sun [e], Zhong-Hua Lu [e,*]

[a] Jiangsu Provincial Key Laboratory of Critical Care Medicine, Department of Critical Care Medicine, ZhongdaHospital, Southeast University, Nanjing, Jiangsu, China
[b] Department of Pulmonary and Critical Care Medicine, Jinan Central Hospital Affiliated to Shandong First Medical University, Jinan, China
[c] Emergency Department of Drum Tower Hospital, The Affiliated Hospital of Nanjing University Medical School, No. 321 Zhongshan Road, Gulou District, Nanjing, China
[d] Department of Ultrasound, Jinan Central Hospital Affiliated to Shandong First Medical University, Jinan, China
[e] The First Department of Critical Care Medicine, The Second Affiliated Hospital of Anhui Medical University, 678 Furong Road, Hefei, Anhui Province, 230601, China

ARTICLE INFO

Handling Editor: Dr Y Renaudineau

Keywords:
Sepsis
Acute respiratory distress syndrome (ARDS)
ANKRD22
Macrophage
Acute lung injury
Inflammatory response

ABSTRACT

Acute respiratory distress syndrome (ARDS) is independently associated with a poor prognosis in patients with sepsis. Macrophage M1 polarization plays an instrumental role in this process. Therefore, the exploration of key molecules affecting acute lung injury and macrophage M1 polarization may provide therapeutic targets for the treatment of septic ARDS. Here, we identified that elevated levels of Ankyrin repeat domain-containing protein 22 (ANKRD22) were associated with poor prognosis and more pronounced M1 macrophage polarization in septic patients by analyzing high-throughput data. ANKRD22 expression was also significantly upregulated in the alveolar lavage fluid, peripheral blood, and lung tissue of septic ARDS model mice. Knockdown of ANKRD22 significantly attenuated acute lung injury in mice with sepsis-induced ARDS and reduced the M1 polarization of lung macrophages. Furthermore, deletion of ANKRD22 in macrophages inhibited M1 macrophage polarization and reduced levels of phosphorylated IRF3 and intracellular interferon regulatory factor 3 (IRF3) expression, while re-expression of ANKRD22 reversed these changes. Further experiments revealed that ANKRD22 promotes IRF3 activation by binding to mitochondrial antiviral-signaling protein (MAVS). In conclusion, these findings suggest that ANKRD22 promotes the M1 polarization of lung macrophages and exacerbates sepsis-induced ARDS.

1. Introduction

Acute respiratory distress syndrome (ARDS) is a common pulmonary disease in Intensive Care Unit (ICU) patients, with a mortality rate of up to 40 % [1]. Sepsis and infection account for 77.5 % of ARDS etiology [2]. ARDS is independently associated with ICU mortality, hospital length of stay (LOS), ICU LOS, and ventilator-free days in patients with sepsis [3]. Activation of immune cells and the resulting uncontrolled inflammation are central to sepsis-induced lung injury [4]. Despite advances in understanding the mechanisms that lead to ARDS, disease-modifying strategies have not improved patient outcomes, resulting in clinical challenges of high mortality and lack of specific drugs [5]. Therefore, it is urgent to explore new therapeutic methods that improve the poor prognosis of septic ARDS patients.

Macrophages are believed to have considerable phenotypic plasticity and functional heterogeneity. Therefore, they are increasingly recognized as key mediators in determining inflammation, injury, and repair programs at each pathological stage of ARDS [6]. Morrell et al. found that the enrichment of "M1-like" (classically activated) and proinflammatory gene expression levels in postmortem ARDS patients progressively increased from Day 1 to Day 28 [7]. Our previous studies also investigated the key genes that simultaneously affect the prognosis of ARDS and the polarization of M1 macrophages[8 9]. Therefore, the aim of this study was to identify key target genes affecting sepsis-induced ARDS using a bioinformatics approach and to explore their mechanisms in acute lung injury as well as macrophage polarization.

In this study, after high-throughput data analysis and validation experiments on two clinical cohorts including 479 patients with sepsis and 34 patients with septic ARDS, interleukin-8 (IL-8) and ankyrin repeat domain-containing protein 22 (ANKRD22) were screened as prognostic molecules that might be simultaneously involved in acute lung injury and M1 polarization. Furthermore, BMDMs (bone marrow-

* Corresponding author.
E-mail addresses: 394873967@qq.com (S. Zhang), liuyao0930@sina.cn (Y. Liu), zhxl_183264@163.com (X.-L. Zhang), sunyun9653@126.com (Y. Sun), luzhonghua@ahmu.edu.cn (Z.-H. Lu).

https://doi.org/10.1016/j.jtauto.2023.100228
Received 14 September 2023; Received in revised form 11 December 2023; Accepted 13 December 2023
Available online 21 December 2023

derived macrophages) that were transfected with shANKRD22 or shIL-8 were used to confirm ANKRD22 as a novel molecular regulator of M1 macrophage polarization. ANKRD22 knockout mice were used to confirm that its role in promoting sepsis-induced lung injury in mice. Subsequent RNA sequencing and molecular experimentation investigating biological pathways revealed that ANKRD22 regulates M1 macrophage polarization by binding to mitochondrial antiviral-signaling protein (MAVS) to activate interferon regulatory factor 3 (IRF3).

2. Materials and methods

This study included four parts: screening key molecules, cell phenotype verification experiments, mouse ARDS model verification experiments, and molecular mechanism experiments (Supplementary materials: Fig. S1 for the study's flow chart).

2.1. Screening candidates

Sepsis-induced ARDS was defined in accordance with the 2012 Berlin definition. This study included two clinical cohorts to screen prognostic molecules in septic ARDS (training and validation cohorts). We used biometric specimens from the intensive care unit of the Academic Medical Centre in Amsterdam, which contained sepsis prognostic data, as a training cohort. This cohort included 479 patients with sepsis and mRNA expression microarrays (GSE65682). We identified genes significantly associated with 28-day mortality using univariate Cox regression analysis ($P < 0.05$). To further explore and screen key genes involved in sepsis and M1-polarized macrophages, the macrophage mRNA expression data were downloaded from the GEO repositories of GSE46903, and the genes with significant differences were identified by differential analysis. Cross-genes that were significantly associated with 28-day mortality as well as with M1 macrophage polarization differential expression were identified, and we further verified the expression of the selected genes in the clinical cohort.

2.2. Inclusion and exclusion criteria for the validation cohort

The validation cohort included 6 healthy volunteers and 34 septic ARDS patients (mild, moderate and severe). Our inclusion criteria were as follows: sepsis as the cause of ARDS, age at least 18 years, and ARDS diagnosis meeting the Berlin standard at the time of the Respiratory and Intensive Care Unit of The Affiliated Central Hospital of Shandong First Medical University from March 2021 to April 2022. The exclusion criteria of the study were as follows: pregnancy, severe chronic obstructive pulmonary disease, refractory shock and age of <18 years or >85 years. The present study was carried out in accordance with the Declaration of Helsinki. The collection of human samples was scrutinized and approved by the Institution Ethics Committee of the Affiliated Central Hospital of Shandong First Medical University (Ethics Committee Approval Number: JNCH2021-194-01).

2.3. BALF specimens and peripheral blood for candidate validation

To verify whether the candidate genes were involved in the clinical response of septic ARDS, we examined the protein expression of target genes in the bronchoalveolar lavage fluid (BALF) and peripheral blood leukocytes of 34 ARDS patients by enzyme-linked immunosorbent assay (ELISA), while only peripheral blood samples of the control group were tested. Patients underwent fiberoptic bronchoscopy under sedation and analgesia. The bronchoscope was inserted into the selected lung segments with obvious inflammation, and 100 ml of normal saline was dripped and aspirated 3 times to collect BALF. Leukocytes were isolated from peripheral blood and BALF by Ficoll gradient centrifugation. The cells were lysed and the concentrations of ANKRD22 and IL-8 in the diluted lysates were determined by ELISA.

2.4. Validation of $ANKRD22^{-/-}$ mice

C57BL/6 (male, aged 8 weeks) specific pathogen-free (SPF) mice (Weitong Lihua Co., Ltd., Beijing, China) were maintained under SPF conditions. During the whole experiment, the SPF animal room and the ultraclean experimental stage were used for animal rearing and experimental procedures, which were performed throughout the experimental process. The Committee on Animal Care and Use of Jinan Central Hospital granted approval for our animal experiments. (Ethics Committee Approval Number: JNCH2021-114).

ANKRD22 knockout (KO) mice (ANKRD22−/−) were obtained from Cyagen Biosciences (China). PCR was used to test the knockout of ANKRD22. The primer pair used was 5′-GCTGCCCTAAAG TCTTTCCTTCC-3' (Forward), 5′-GGGAGTATCGCC ATTGAAGCTATCT-3' (Reverse). The fragment size was 383 bp and the annealing temperature was 57 °C. The amplified products were purified and analyzed by DNA sequencing. Homozygous $ANKRD22^{-/-}$ mice were used for breeding and subsequent experiments, and wild-type (WT) mice were used as the control group. Genomic DNA was extracted from mouse tail tissue, and specific bands were identified by PCR. BMDMs were obtained from the parental control and $ANKRD22^{-/-}$ mice, and some of the BMDMs from the $ANKRD22^{-/-}$ mice were transfected using ANKRD22 overexpression plasmids for the rescue experiments. The expression of ANKRD22 in each group of macrophages was subsequently verified by PCR and Western blotting (Supplementary materials: Fig. S2 for verification results).

2.5. The construction of septic ARDS models

The main cause of ARDS is sepsis [10], which may be caused by pulmonary or extrapulmonary infection [11]. Therefore, we used two septic ARDS animal models in the current study: pulmonary ARDS caused by intratracheal injection of lipopolysaccharide (LPS) and extrapulmonary ARDS caused by cecal ligation and puncture **(**CLP). The LPS-induced septic ARDS mouse model was established as described in our previous study [12]. Briefly, mice were anesthetized by intraperitoneal injection of pentobarbital and were subjected to transtracheal injection of LPS (5 mg/kg) (Sigma−Aldrich). To construct the CLP-induced septic ARDS model, mice were anesthetized with intraperitoneal injection of pentobarbital, shaved, disinfected, and incised, and the cecum was exposed, ligated, and punctured with a 22-gauge needle. The needle was pushed to remove the fecal material from the hole, and the abdominal incision was sutured. ARDS-Sham mice were treated with the same amount of normal saline (0.9 %) without anesthetics.

2.6. Experimental groups and sample acquisition

To investigate the change in lung ANKRD22 expression during septic ARDS, mice were randomly divided into the LPS group, CLP group and sham group (6 mice in each group). The specific methods of ARDS modeling are described above, and the mice in each group were sacrificed 24 h after modeling. Lung tissue was gathered for single cell isolation and histological examination as previously described with slight modifications [13].

Following the observation that pulmonary ANKRD22 expression was upregulation in sepsis ARDS, we investigated the effect of ANKRD22 knockout on sepsis-induced ARDS. Mice were assigned randomly to either of the following groups (n = 6 mice per group): ①② LPS-WT and CLP-WT groups. The procedure was performed according to the mouse model of "LPS-induced septic ARDS" and "CLP-induced septic ARDS", respectively. ③④In the LPS-Sham and CLP-Sham groups, the procedure was performed according to the ARDS-Sham mouse model. ⑤⑥In the LPS-KO and CLP-KO groups, the procedure was performed according to the mouse model of "LPS-induced septic ARDS" and "CLP-induced septic ARDS", but $ANKRD22^{-/-}$ mice were used. The mice in each group were sacrificed 24 h after modeling.

2.7. Cytokine analysis by ELISA

The culture supernatant of mouse BALF and macrophages, as well as diluted leukocyte lysates from human BALF and peripheral blood samples, were collected, and enzyme-linked immunosorbent assay was used to measure the concentration of some or all of the following proteins: ANKRD22 (ELISA, Aoxing, AX100086H), interleukin-8 (IL-8) (ELISA, Abcam, ab214030), chemokine ligand 2 (CCL2) (ELISA, R&D Systems, MJE00B), interleukin-1 β (IL-1β) (ELISA, Abcam, ab197742), interleukin-6 (IL-6) (ELISA, Abcam, ab222503) and interferon-beta (IFN-β) (ELISA, Abcam, ab252363).

2.8. Evaluation of lung histopathology and pulmonary edema

The right upper lobe was encapsulated in paraffin and sagittally sectioned into 5-μm-thick sections. Sections were treated with hematoxylin and eosin staining. Alveolar and interstitial inflammatory cell infiltrates, hemorrhage, edema, atelectasis and hyaline membrane formation were individually rated on a scale of 0–4. The degree of severity of lung injury was measured as the sum of the scores [14]. The proportion of lung wet weight to body weight (LWW/BW) was calculated for each group of mice to indicate the degree of pulmonary vascular permeability and the severity of pulmonary edema.

2.9. Isolation and culture of bone marrow-derived macrophages

Wild-type or ANKRD22$^{-/-}$ mouse BMDMs were generated as previously described with minor modifications. BMDMs were extracted from the medullary cavity of the femur and tibia on a superclean bench. The erythrocytes were lysed using lysing buffer (BD Pharm Lyse™, USA), and the remaining cells were washed three times in phosphate-buffered saline (PBS) and then cultured in fresh DMEM containing 10 % FBS and 20 ng/ml *M*-CSF for 7 days in a humidified 5 % CO_2 sterile incubator at 37 °C. Flow cytometry was used to detect F4/80 for the identification of BMDMs.

2.10. Construction and transduction of lentiviral vectors of ANKRD22-RNA/shRNA, IL-8-shRNA and MAVS-shRNA

Lentiviral vectors were used to achieve low and high expression of ANKRD22 and low expression of IL-8 and MAVS genes, while overexpression and low expression of empty lentivirus were used as negative controls. The lentiviruses were packaged in 293 T cells (Cyagen Biosciences, Inc.) with the aid of three packaging plasmids, and then the lentivirus titer was measured. Finally, the most efficient sequence of shRNA-ANKRD22 was identified as GGAGAAATGCTGATGTCAACC, the most efficient sequence of shRNA-IL-8 was GCAATGAAGCTTCTGTATAGT, and the most efficient sequence of shRNA-MAVS was GCTGAGGACAAGACCTATAAG. Similarly, we constructed ANKRD22-overexpressing lentiviral plasmids and control empty vector lentiviral plasmids (Xhol-ANKRD22-F: ATACTCGAGCGATGGGAATCCTATATTCT GAGCCCA, NotI-ANKRD22-R: ATAGCGGCCGCTGATTACGATTTCTCT CGGAGGATC; Xhol-IL-8 –F: ATACTCGAGCGATGGCTGCTCAAGGCTG GTCCATGC, NotI-IL-8-R: ATAGCGGCCGCCTTCAGTCGAACTGTCCGTCACTACGGATT). (Supplementary materials: Fig. S3 for details).

BMDMs from passages 1–4 were used for transduction and the ANKRD22, IL-8, and MAVS overexpression and knockdown experiments. ANKRD22 gene overexpression and downregulated expression were achieved using lentiviral vectors, and lentiviruses for overexpression and downregulated expression were used as negative controls. Constructs expressing the shRNAs targeting endogenous ANKRD22, IL-8 and MAVS were encoded into the lentiviral vector and transfected into BMDMs with lentivirus supernatant (infection multiple = 50). Three days after transfection, the expression of ANKRD22, IL-8 and MAVS protein was detected by Western blot to evaluate the effect of shRNA after infection. The AKNDR22 overexpression vector and an empty vector were transfected into BMDMs, and western blotting was used to detect the expression of ANKRD22 protein in the BMDMs of each group to evaluate the overexpression effects after transfection. (Supplementary materials: Fig. S4 for details).

2.11. Construction of the polarization model of M1-type macrophages

The polarization model of M1-type macrophages was constructed by using LPS and poly (I:C) inducers. Lipopolysaccharide, a cell wall product of gram-negative bacteria, is a common inducer of septic ARDS and has been widely used to construct M1 polarization models [15, 16]. In this study, it was found that the Rig-I pathway is the molecular mechanism by which ANKRD22 regulates M1 polarization, and poly (I:C) is an activator of the Retinoic acid-inducible gene I (RIG-I) pathway [17]. Therefore, poly (I:C) was used to induce the polarization model of M1 macrophages [9, 18].

2.12. Immunohistochemical staining

Lung sections were deparaffinized and hydrated. The sections underwent antigen retrieval at a high temperature and were blocked for 1 h using 5 % goat serum. After blocking, the sections were incubated overnight at 4 °C with primary antibodies (diluted 1:100). The primary antibodies used were against F4/80 (F4/80: BD Pharmingen™, RatmAb #746070). After incubation, the sections were washed 3 times with PBS and incubated with a 1:50 dilution of biotinylated secondary antibody. The reaction products were incubated with diaminobenzidine (DAB, China) and then counterstained with hematoxylin. Positive areas were quantified with ImageJ. All images were captured under high-power magnification (× 200) using a light microscope (Olympus).

2.13. Flow cytometry

For phenotypic analysis of cell surface marker expression, cultured BMDMs and lung single-cell suspensions were resuspended in PBS, incubated for 15 min with FcR blocking reagent, and then incubated for 15 min with a PE-conjugated anti-mouse CD86 (BD Pharmingen™, Mouse Anti-Rat Ab #555016) or FITC-conjugated anti-mouse F4/80 (F4/80: BD Pharmingen™, RatmAb #746070) antibody following the manufacturers' instructions. F4/80 was utilized to identify macrophages, and CD86 was utilized as the marker of M1 macrophages. The expression of CD86 was calculated from the fluorescence intensity. The stained cells were washed twice, resuspended in cold buffer and then analyzed by flow cytometry (ACEA NovoCyte, China), and the results were processed using FlowJo software version X (Tree Star, USA).

2.14. Polymerase chain reaction (PCR)

Total cellular RNA was extracted from cells using TRIzol reagent. cDNA was synthesized from 2 μg of total ANKRD22 using *M*-MLV reverse transcriptase (Gibco-BRL, Gaithersburg, MD). cDNA for ANKRD22 and GAPDH was amplified by PCR with specific primers. PCR products were analyzed using agarose gel electrophoresis.

Agarose gel electrophoresis was used to identify the genomic DNA fragments of the tail samples from transgenic mice. DNA extracted from the transgenic and parental lines was digested with *Eco*RV restriction enzyme, and 1.0 % agarose gel was used. Then, 0.20 g agarose and 20 ml 1*X* Tris-acetate-EDTA buffer in a flask were heated in a microwave for 5 min at 100 °C. Then, 2 μl of ethidium bromide was added (Thermo Fisher Scientific, Inc. And poured onto a taped plate with casting combs. Then, 2 μl of mouse tail DNA samples or macrophage DNA samples were added to a 5*X* agarose gel and subjected to electrophoresis at 120 mA for 40 min at 25 °C until separation was achieved. The DNA fragments were observed by a Bio-Rad gel imager.

2.15. Western blot (WB) analysis

For ANKRD22 downstream molecular analysis, the expression levels of ANKRD22, inducible nitric oxide synthase (iNOS), total IRF3, IRF3, *p*-IRF3, nuclear IRF3, histone-3, IL-8, MAVS, GAPDH, and b-tubulin were evaluated by Western blot analysis. Proteins were separated by sodium dodecyl sulfate–polyacrylamide gel electrophoresis and transferred to polyvinylidene difluoride (PVDF) membranes. The membranes were incubated with primary antibodies against ANKRD22, iNOS, IRF3, *p*-IRF3, histone-3, IL-8, MAVS and RIG-I at 4 °C overnight. The membranes were incubated with secondary antibody for 1 h at room temperature. The immunoblots were visualized using enhanced chemiluminescence (ECL; Thermo Scientific). The expression levels from whole cell extracts were normalized against that of β-tubulin. The following antibodies were used for western blotting in the current study:

ANKRD22: Invitrogen, rabbit mAb #PA5-71839;

iNOS: Abcam, rabbit mAb #EPR16635;

IRF3: Abcam, rabbit mAb #EPR2418Y;

p-IRF3: Cell Signaling Technology, rabbit mAb #29047;

Histone-3: Abcam, Mouse mAb #mAbcam6002;

IL-8: Abcam, rabbit mAb #EPR14470;

MAVS: Abcam, rabbit mAb #ab31334;

RIG-I: Cell Signaling Technology, rabbit mAb #4200; Melanoma-differentiation-associated gene 5 (MDA5): Cell Signaling Technology, rabbit mAb #5321

β-Tubulin: Abcam, rabbit mAb #EPR1330.

2.16. Coimmunoprecipitation

We used a coimmunoprecipitation method to identify proteins that might be associated with the proteins of interest. The cells were lysed with extraction buffer, sonicated and cleared by centrifugation at 14,000×*g* for 10 min at 4 °C. The protein level was normalized with a protein assay kit (Bio-Rad Laboratories, USA). The supernatant was incubated overnight at 4 °C with 1:250 dilutions of the primary antibody. Protein A/G agarose (Beyotime) was added and incubated for an additional 4 h at 4 °C. After washing, the proteins were boiled in SDS sample buffer. These samples were subjected to immunoblotting with antibodies against RIG-I, MDA5, MAVS and ANKRD22 according to the manufacturer's instructions.

2.17. RNA-seq

Total RNA was prepared from ANKRD22-BMDMs and control ANKRD22-BMDMs by TRIzol. After removing the rRNA, the total RNA was prepared according to Illumina's instructions. The libraries were sequenced using Illumina Sequencing Technology on an Illumina Genome Analyzer II according to the manufacturer's instructions [19, 20].

2.18. Gene set enrichment analysis

To gain insight into the mechanisms underlying the regulatory role of ANKRD22, transcriptome II sequencing was utilized to determine all-gene expression in ANKRD22-overexpressing BMDMs and Ctrl-BMDMs. Gene set enrichment analysis (GSEA) was conducted to explore downstream pathways. GSEA has been shown to provide increased sensitivity to detect small changes in gene expression within specific sets of functionally related genes, which have been described in detail in our previous work [9]. To confirm our bioinformatics predictions, phosphorylation and nuclear protein western blotting were performed to study the key features of the activated enrichment pathways in macrophages, transfected macrophages, and control cells.

2.19. Statistical analysis

Univariate Cox proportional hazards regression with Bonferroni correction was used for multiple comparisons and mRNAs associated with sepsis prognosis were identified using the survival R package, with a cutoff value of $P < 0.05$. We screened genes that were significantly differentially expressed between M1 macrophages and M0 and M2 macrophages (2-fold difference, $FDR < 0.05$) to identify genes that might be involved in the polarization of M1 macrophages. In the high-throughput experiments, $FDR < 0.05$ was defined as the cutoff value. The statistics and algorithms of the high-throughput experiments are described in the analysis of the high-throughput sequencing. For western blotting, ELISA and flow cytometry, $P < 0.05$ was defined as a significant result. The testing results were analyzed by using one-way ANOVA in R 4.0.3 software.

3. Results

3.1. Screening for genes associated with macrophage M1 polarization and sepsis patient prognosis and validating their expression in ARDS patients

The training cohort included 479 patients with sepsis and all mRNA expression microarrays. A total of 1182 transcripts were screened as prognostic molecules in sepsis patients and were significantly associated with 28-day cumulative mortality (all $P < 0.05$). To investigate the genes potentially involved in M1 macrophage polarization, a secondary analysis was performed on the macrophage polarization dataset (transcript counts for each subtype of macrophage:M0 47, M1 38, M2 40). We identified 100 significantly differentially expressed genes between M1 macrophages and M0 and M2 macrophages [2-fold difference, false discovery rate (FDR) < 0.05)]. Furthermore, to find candidate genes simultaneously associated with the prognosis of sepsis patients and M1 macrophages, a Venn diagram was plotted to capture the overlap between the 1182 transcripts significantly associated with sepsis patient 28-day mortality and the 100 genes specifically expressed in M1 macrophages (Fig. 1A). Finally, 8 candidate genes, including potassium inwardly rectifying channel subfamily J member 2 (KCNJ2), IL-8, transmembrane protein 140 (TMEM140), purinergic receptor P2X 7 (P2RX7), CD93, interferon regulatory factor 1 (IRF1), syntaxin 11 (STX11) and ANKRD22, which were both associated with sepsis and expressed in M1-polarized macrophages (all $P < 0.05$), were screened out (Fig. 1A). Cox regression analysis of 28-day mortality and sepsis gene expression was conducted, and forest plots were used to illustrate the HR of these 8 candidate genes (all $P < 0.05$).

The expression of the IL-8 and ANKRD22 genes was significantly upregulated in sepsis patients with a poor prognosis, suggesting that these two genes may be involved in sepsis-induced ARDS. IL-8 and ANKRD22 were identified as risk molecules with HRs of 1.33, (95 % CI: 1.05, 1.68) and 2.70, (95 % CI: 1.75, 4.16), respectively (Fig. 1B). The heatmap shows that the expression of IL-8 and ANKRD22 was markedly upregulated in M1-polarized macrophages (Fig. 1C).

To further verify whether there were differences in the expression of IL-8 and ANKRD22 in septic ARDS patients with different severities, we evaluated these two proteins in the peripheral blood and alveolar lavage fluid of ARDS patients with different severities. The validation cohort included 6 healthy volunteers and 34 septic ARDS patients, including 8 mild patients, 12 moderate patients and 14 severe patients. The details of the patient information are shown in Table 1 (Supplementary materials: Table 1 for details). BALF was collected from 21 septic ARDS patients, and peripheral blood specimens were collected from all participants. The ELISA results showed that the levels of IL-8 and ANKRD22 in the peripheral blood of ARDS patients were significantly increased compared with those in the peripheral blood of volunteers. The levels of IL-8 and ANKRD22 in the BALF and peripheral blood of severe patients was significantly higher than those in the BALF and peripheral blood of mild or moderate patients (Fig. 1D and E).

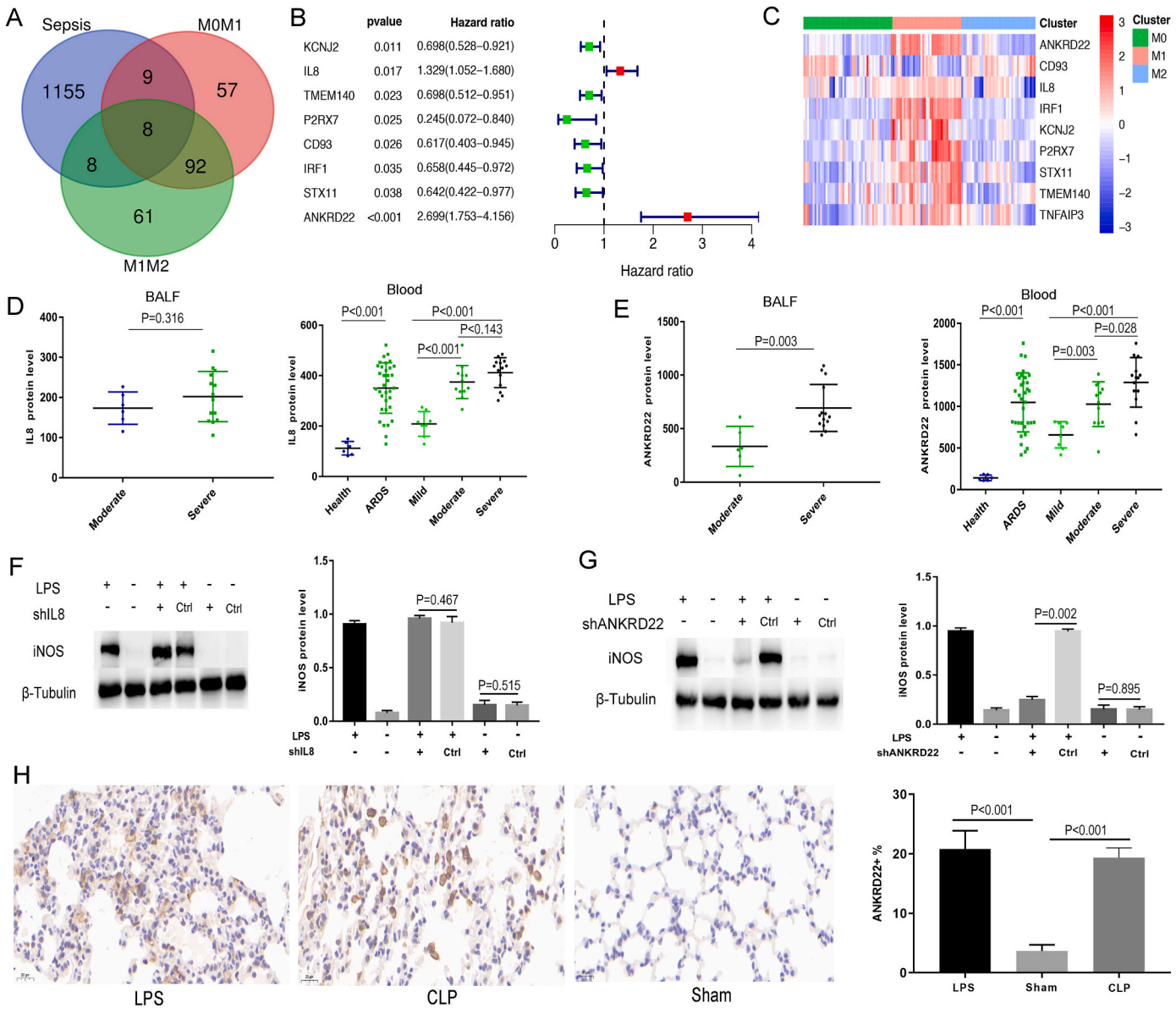

Fig. 1. Screening for genes associated with macrophage M1 polarization and sepsis patient prognosis and validating their expression in ARDS patients A. Eight molecules were screened as molecules associated with M1 polarization and sepsis patient prognosis. B. Forest plots of these 8 molecules. Through Cox regression analysis of 28-day mortality in sepsis patients and gene expression, high IL-8 and ANKRD22 expression was identified as a risk factor associated with poor septic patient prognosis. C. The expression of 8 molecules in M0/M1/M2-polarized macrophages. IL-8 and ANKRD22 were upregulated in M1 macrophages compared with M0 and M2 macrophages, *FDR* <0.05. D. Expression of IL-8 in the peripheral blood and alveolar lavage fluid of ARDS patients. E. Expression of ANKRD22 in the peripheral blood and alveolar lavage fluid of ARDS patients. F. WB was used to detect the effect of low IL-8 expression on iNOS protein expression in macrophages under different conditions. G. WB was used to detect the effect of low ANKRD22 expression on iNOS protein expression in macrophages under different conditions. H. Detection of ANKRD22 expression in the lung tissue of pulmonary and extrapulmonary septic ARDS model mice by immunohistochemical staining. (In Figure F, G and H, n = 3, each experiment was repeated times. All data are expressed as mean ± SD).

iNOS, which reflects M1 polarization of macrophages, is closely related to ALI [21, 22]. To further investigate whether IL-8 and ANKRD22 may regulate iNOS expression, and therefore macrophage M1 polarization, shRNA was used to knockdown the expression of IL-8 and ANKRD22 in BMDMs. We found that the expression of iNOS was significantly upregulated after LPS-induced M1 polarization of macrophages, which was not significantly changed in the LPS + shIL-8 group but was obviously downregulated in the LPS + shAKNRD22 group (Fig. 1F and G). Further immunohistochemical experiments showed that ANKRD22 was markedly upregulated in lung tissue cells of CLP-ARDS and LPS-ARDS model mice compared with sham mice (Fig. 1H). These results suggest that AKNRD22 may be a key gene affecting ARDS occurrence and M1 macrophage polarization.

3.2. *ANKRD22 contributes to LPS-induced M1 macrophage polarization*

Is AKNRD22 a key gene that regulates the polarization of M1 macrophages? To resolve this question, we first evaluated the effect of AKNRD22 on the expression of iNOS and the M1 polarization marker CD86 in macrophages. Compared with the unstimulated macrophages, the AKNRD22-highly expressed macrophages exhibited significantly upregulated iNOS protein expression and a significantly increased mean fluorescence intensity (MFI) of CD86. In the LPS microenvironment, the protein expression (MFI) of CD86 and iNOS in macrophages with high AKNRD22 expression was also markedly upregulated (Fig. 2A and B). The secretion levels of inflammatory cytokines was measured by ELISA, which showed that IL-1β, IL-6 and CCL2 levels were increased in the

Table 1
Baseline Characteristics of enrolled patients.

Characteristics	Mild (n = 8)	Moderate (n = 12)	Severe (n = 14)	*P*
Age — yr (mean ± SD)	55.50 ± 14.08	59.92 ± 15.65	47.14 ± 14.71	0.103
Gender — Male no./total no.	5/8	6/12	9/14	0.750
Primary cause of lung injury — no./total no.	6/8	11/12	12/14	0.702
APACHE III score (mean ± SD)	79.75 ± 22.76	93.08 ± 27.19	101.90 ± 24.56	0.156
Shock at baseline —no./total no.	6/8	7/12	11/14	0.629
Systolic BP (mmHg) (mean ± SD)	115.00 ± 16.48	107.60 ± 18.37	113.57 ± 15.32	0.551
Diastolic BP (mmHg) (mean ± SD)	55.00 ± 16.32	53.91 ± 9.25	68.21 ± 14.25	0.019
Tidal volume — ml/kg of predicted body weight [Median (IQR)]	6.08 (5.88, 6.92)	6.04 (5.98, 7.02)	6.08 (5.88, 6.92)	0.867
Minute ventilation — liters/min (mean ± SD)	9.12 ± 2.42	10.17 ± 3.59	10.17 ± 2.11	0.695
Mean airway pressure (cm H2O) (mean ± SD)	14.75 ± 6.14	12.42 ± 4.38	16.64 ± 3.57	0.075
PEEP — cm of water [Median (IQR)]	6.00 (5.00, 10.00)	5.00 (5.00, 8.00)	12.00 (8.00,14.00)	0.044
PaCO2 — mmHg [Median (IQR)]	43.00 (34.50, 52.00)	36.50 (30.00, 49.00)	36.00 (31.50,41.50)	0.292
PaO2:FiO2 — mmHg [Median (IQR)]	237.50 (221.80, 257.50)	156.50 (134.00, 173.50)	75.00 (68.575,81.75)	<0.001
Creatinine — mg/dl [Median (IQR)]	1.00 (0.25, 1.75)	1.00 (1.00,2.00)	1.00 (0.75,2.00)	0.402
Creatine kinase — U/liter [Median (IQR)]	54.00 (19.00, 333.00)	42.50 (28.00,210.00)	130.50 (50.75,297.00)	0.339
Alanine aminotransferase — U/liter (mean ± SD)	31.50 ± 23.77	28.00 ± 22.26	38.29 ± 23.20	0.519
Aspartate aminotransferase — U/liter (mean ± SD)	50.63 ± 42.12	42.58 ± 27.03	54.71 ± 32.50	0.650

Results are given as mean ± SD or median [IQR]. IQR: interquartile range.

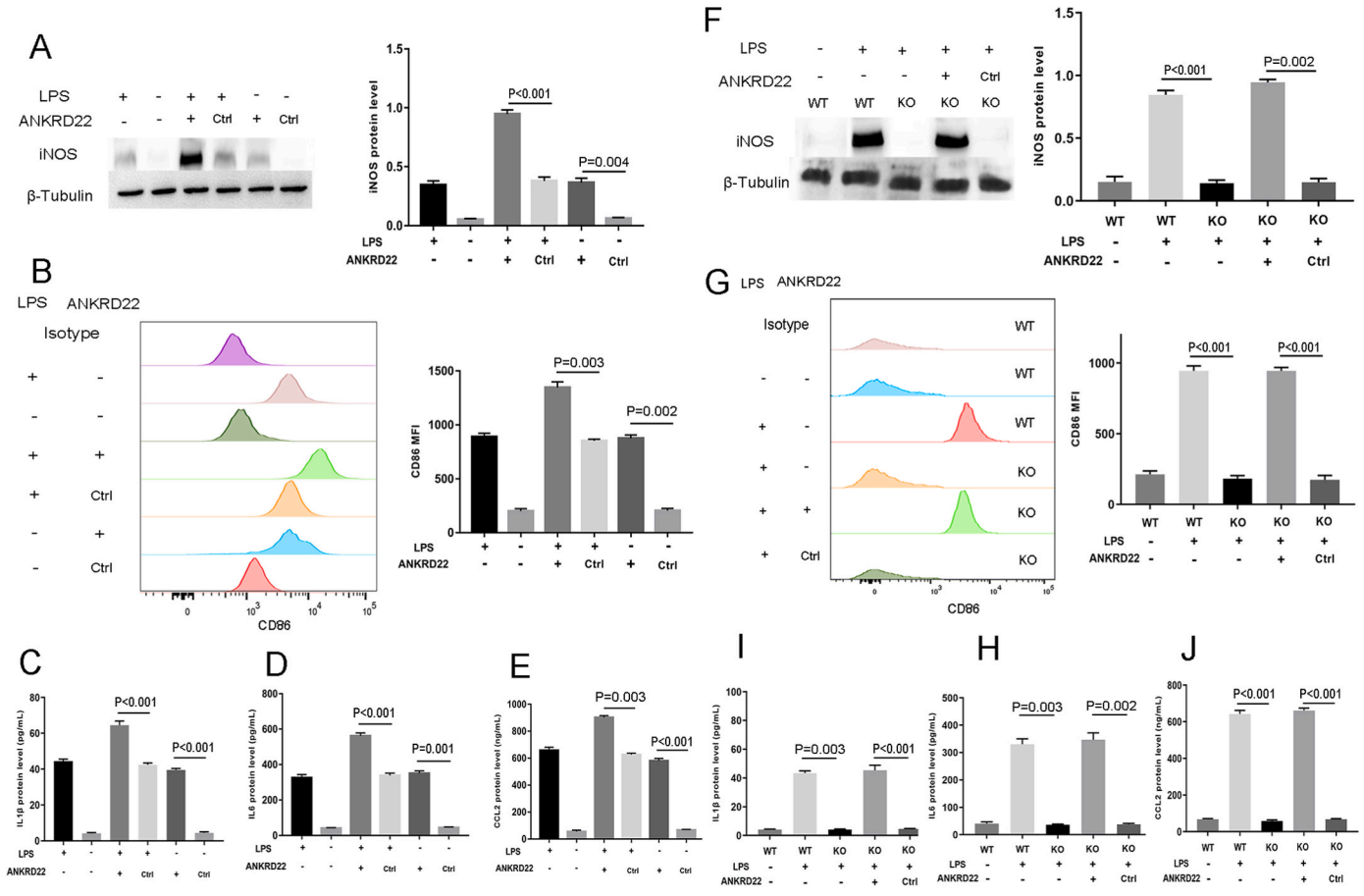

Fig. 2. ANKRD22 contributes to macrophage M1 polarization A. WB was used to detect the effects of ANKRD22 overexpression on iNOS protein expression in macrophages under different conditions. B. Flow cytometry was used to evaluate the effect of ANKRD22 overexpression on the MFI of CD86 in macrophages. *C*-E. ELISA was used to evaluate the effect of ANKRD22 overexpression on the macrophage secretion levels of proinflammatory the cytokines IL-1β, IL-6 and CCL2 F. Flow cytometry was used to evaluate the effect of ANKRD22 knockdown on the MFI of CD86 in macrophages G-I. ELISA was used to evaluate the effect of ANKRD22 knockdown on the macrophage secretion levels of the proinflammatory cytokines IL-1β, IL-6 and CCL2. (n = 3, data are expressed as mean ± SD, each experiment was repeated three times).

AKNRD22-overexpressing group after lipopolysaccharide stimulation (Fig. 2C–E). However, validation using ANKRD22$^{-/-}$ mouse-derived macrophages revealed a significant downregulation in iNOS and CD86 expression as well as IL-1β, IL-6 and CCL2 secretion levels by LPS-stimulated macrophages after ANKRD22 deletion (Fig. 2F–J). Rescue experiments using ANKRD22 knockdown macrophages transfected with

the ANKRD22 high expression plasmid showed that the expression levels of INOS and CD86 increased again after LPS stimulation (Fig. 2F and G). In the above rescue experiment, the levels of the proinflammatory factors IL-1β, IL-6 and CCL2 also showed similar changes (Fig. 2I and J). These results indicate that AKNRD22 is an important gene that determines the progression of macrophage polarization toward the M1 phenotype.

3.3. ANKRD22 plays an important role in sepsis-induced ARDS

To further verify the role of ANKRD22 in sepsis-induced ARDS, we knocked out the ANKRD22 gene in mice and established a septic ARDS model and then separately evaluated the effect of ANKRD22 on lung injury in septic ARDS caused by pulmonary and extrapulmonary infection. We used a histological evaluation of the lungs to confirm the effect of ANKRD22 on LPS/CLP-induced lung injury in mice. Compared with the control mice, the LPS and CLP model mice showed acute lung injury; that is, the pathological specimens showed extensive thickening of the alveolar wall and obvious infiltration of inflammatory cells in the LPS-WT/CLP-WT group, whereas knockdown of ANKRD22 attenuated these changes in the LPS-KO/CLP-KO group (Fig. 3A). The lung injury scores in the LPS- KO and CLP-KO groups were significantly lower than those in the LPS-WT and CLP-WT groups, respectively (Fig. 3A–B).

The LWW/BW response to pulmonary edema is related to the severity of lung injury. In the endogenous or exogenous LPS- or CLP-induced ARDS model mice, the LWW/BW ratio was significantly higher than that in the control group. After ANKRD22 was knocked out, the LWW/BW ratio was significantly reduced in mice with LPS-induced pulmonary ARDS or CLP-induced extrapulmonary ARDSFig. 3C), suggesting that ANKRD22 knockout can effectively inhibit lung injury and alleviate ARDS.

Cytokine storm-mediated lung injury is an important mechanism of ARDS [23]. In this study, the levels of IL-1β, IL-6 and CCL2 in the alveolar lavage fluid of the LPS- or CLP-induced pulmonary and extrapulmonary ARDS model mice were significantly higher than those in the alveolar lavage fluid of the control mice. Knockout of ANKRD22 inhibited the production of the pulmonary or extrapulmonary ARDS proinflammatory cytokines IL-1β, IL-6 and CCL2 (Fig. 3d and e). These results indicate that high expression of ANKRD22 is critically linked to the ARDS inflammatory storm and exacerbation of lung injury.

3.4. ANKRD22 promotes the M1 polarization of macrophages in ARDS model mice

Previous studies have shown that macrophage M1 polarization contributes to particulate matter (PM)-induced lung injury [24], while inhibition of M1 polarization can alleviate acute lung injury [25]. Therefore, we evaluated the effect of ANKRD22 knockout on the ratio of M1-type macrophages in the lungs of ARDS model mice using immunohistochemistry and flow cytometry. Compared with the that in the lungs of the LPS-Sham group, the proportion of $F4/80^{+}$ macrophages in the lungs of LPS-induced ARDS model mice was significantly increased. After ANKRD22 knockout, the proportion of F4/80+ macrophages in the lungs of mice was significantly reduced again (Fig. 4A and B). ANKRD22 knockdown had a similar effect on CLP-induced ARDS model mice (Fig. 4A and B), further suggesting that ANKRD22 promotes M1-type macrophage aggregation in the lungs during sepsis-induced ARDS.

We have demonstrated that ANKRD22 regulates the M1 polarization of macrophages in vitro and that ANKRD22 expression is upregulated in ARDS model mice in vivo. Here, we further prove that ANKRD22 has an effect on the M1 polarization of macrophages in ARDS model mice. Flow

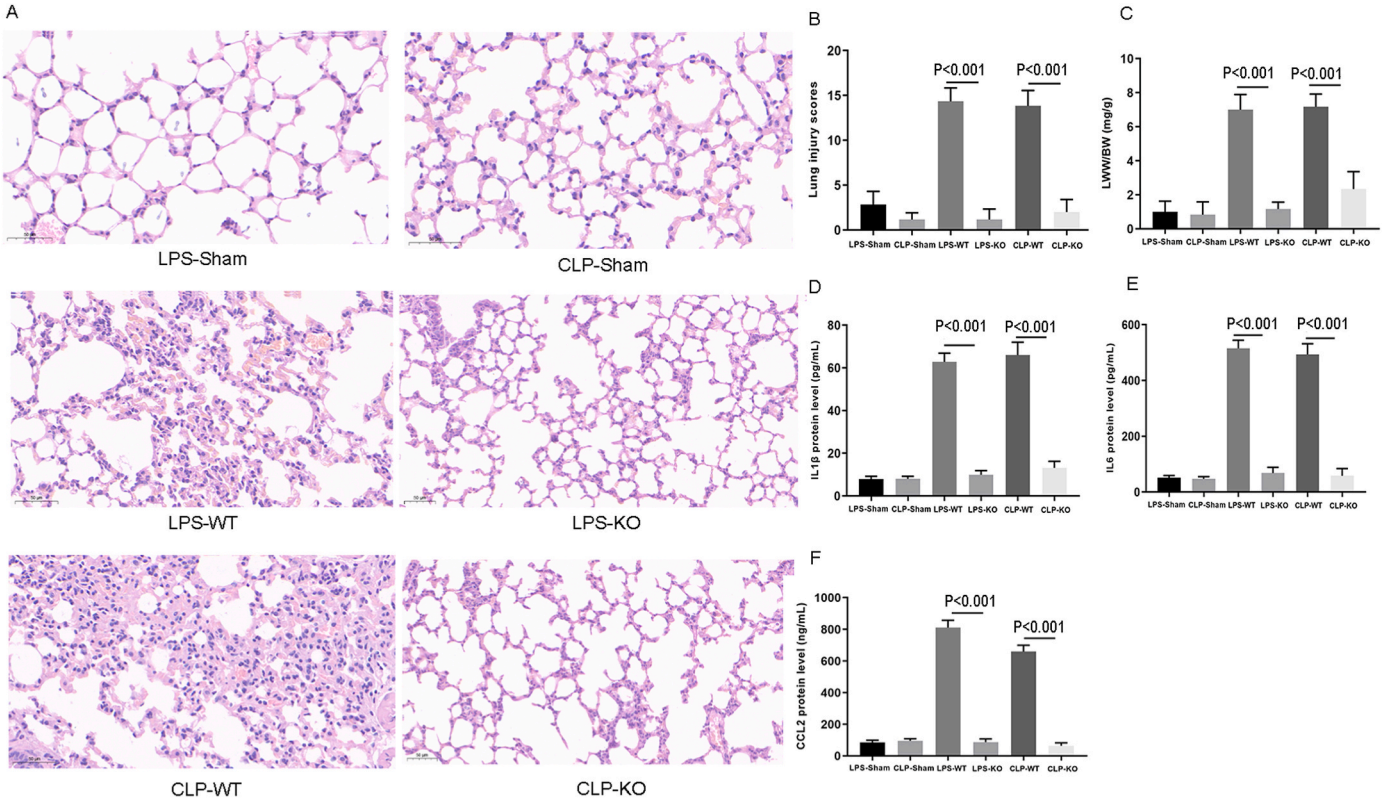

Fig. 3. AKNRD22 plays critical roles in sepsis-induced ARDS A. Representative histological sections of lung tissue from ARDS model mice 24 h after modeling (hematoxylin and eosin staining; magnification, × 200). B. The pathological lung injury score based on histological sections. C. Comparison of the lung wet weight to body weight ratio (LWW/BW) in different groups at 24 h. D. Comparison of the proinflammatory cytokine IL-1β levels in alveolar lavage fluid by ELISA. E. Comparison of the proinflammatory cytokine IL-6 levels in alveolar lavage fluid by ELISA. F. Comparison of the proinflammatory cytokine CCL2 levels in alveolar lavage fluid by ELISA. Data are expressed as the mean ± SD. (n = 6, data are expressed as mean ± SD, each experiment was repeated three times).

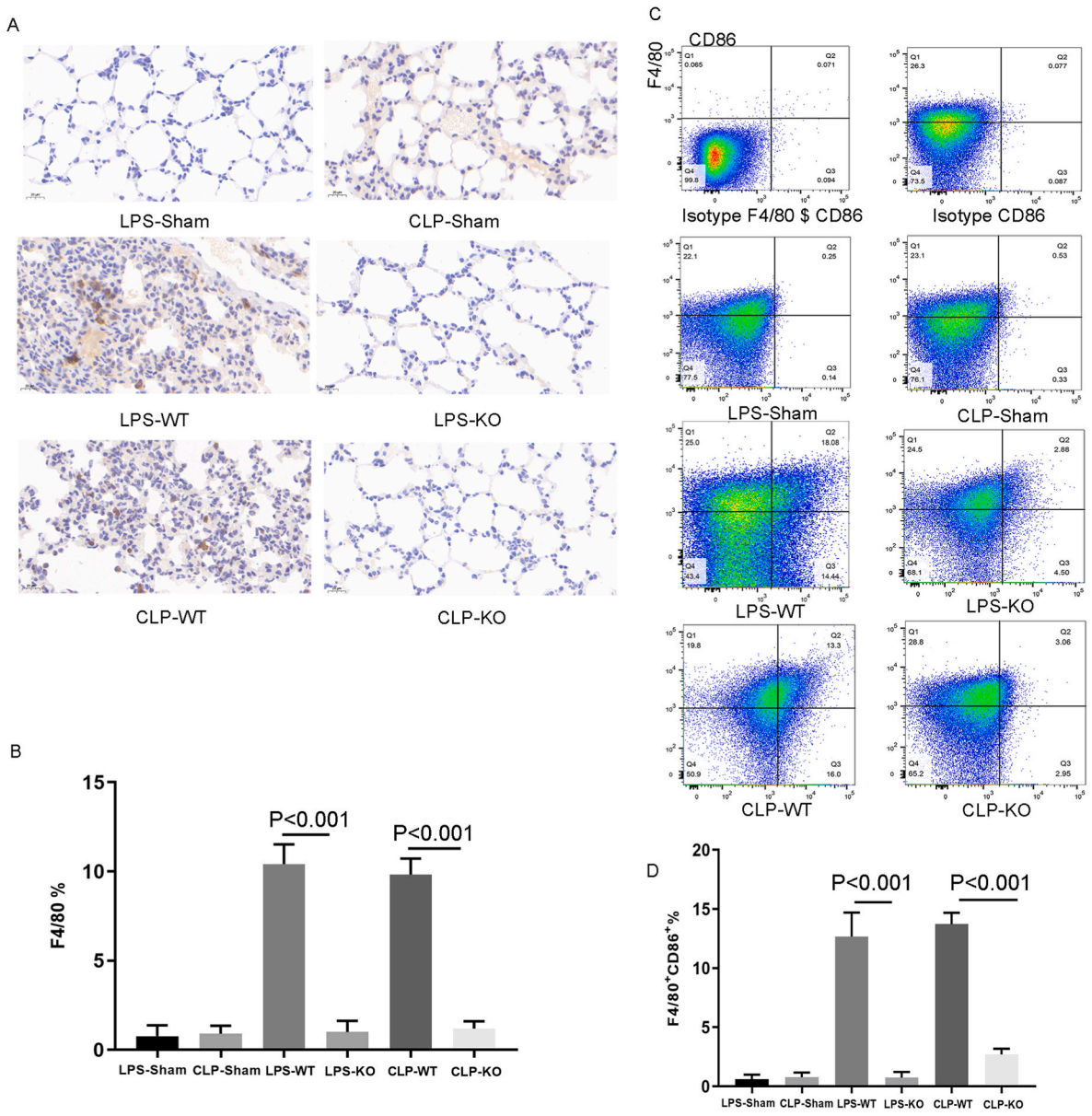

Fig. 4. ANKRD22 promotes M1 polarization of macrophages in ARDS model mice A. Immunohistochemical staining for F4/80 in the lung tissues of different groups. B. Comparison of the proportion of F4/80+ cells in the lung tissues of each group. C. Representative flow scatter plots of CD86 + F4/80+ single lung cells in each group. D. The histogram shows the percentage of CD86 + F4/80+ cells in single lung cells in each group. (n = 6, data are expressed as mean ± SD, each experiment was repeated three times).

cytometry results showed that the CD86 expression of macrophages was significantly upregulated in the lung tissue of LPS-ARDS or CLP-ARDS model mice, while the M1 polarization of macrophages in the lungs of both groups was significantly decreased after ANKRD22 knockdown (Fig. 4C and D). These findings indicate that ANKRD22 promotes the development of ARDS and regulates macrophage M1 polarization, but the mechanism is not clear.

3.5. *ANKRD22 promotes macrophage M1 polarization by activating IRF3*

To explore the underlying mechanism by which ANKRD22 regulates macrophage M1 polarization, transcriptome II sequencing was utilized to detect all-gene expression in ANKRD22-BMDMs and Ctrl-BMDMs. GSEA showed that RIG-I might be the underlying signaling pathway (*FDR* < 0.05) (Supplementary materials: Fig. S5 for details). Rig-I receptors are cell sensor proteins that activate signaling cascades that lead to the production of the proinflammatory cytokine IFN-β [26].

RIG-I pathway activation is characterized by IRF3 phosphorylation and IRF3 translocation into the nucleus, and these events have been shown to promote macrophage M1 polarization in our previous studies [8]. Western blotting of subcellular fractions was performed to validate whether ANKRD22 could affect poly (I:C)-induced IRF3 activation. Compared with the macrophage cells in the control group, the macrophage cells in the high expression ANKRD22 group showed significantly increased phosphorylated IRF3 and IRF3 levels in the nucleus, with or without the poly (I:C) stimulation (Fig. 5A and B). After receiving poly (I:C) stimulation, IRF3 activation was increased in macrophages extracted from wild-type mice but significantly decreased in the ANKRD22-KO group, which was again increased in the overexpression ANKRD22 rescue experiment (Fig. 5D–F).

Rig-I receptors activate and upregulate the expression of the sepsis proinflammatory factor IFN-β [27–29], so inhibition of the IRF3 signaling pathway may reduce the inflammatory response in sepsis [30]. In this study, compared with the control group, the ANKRD22

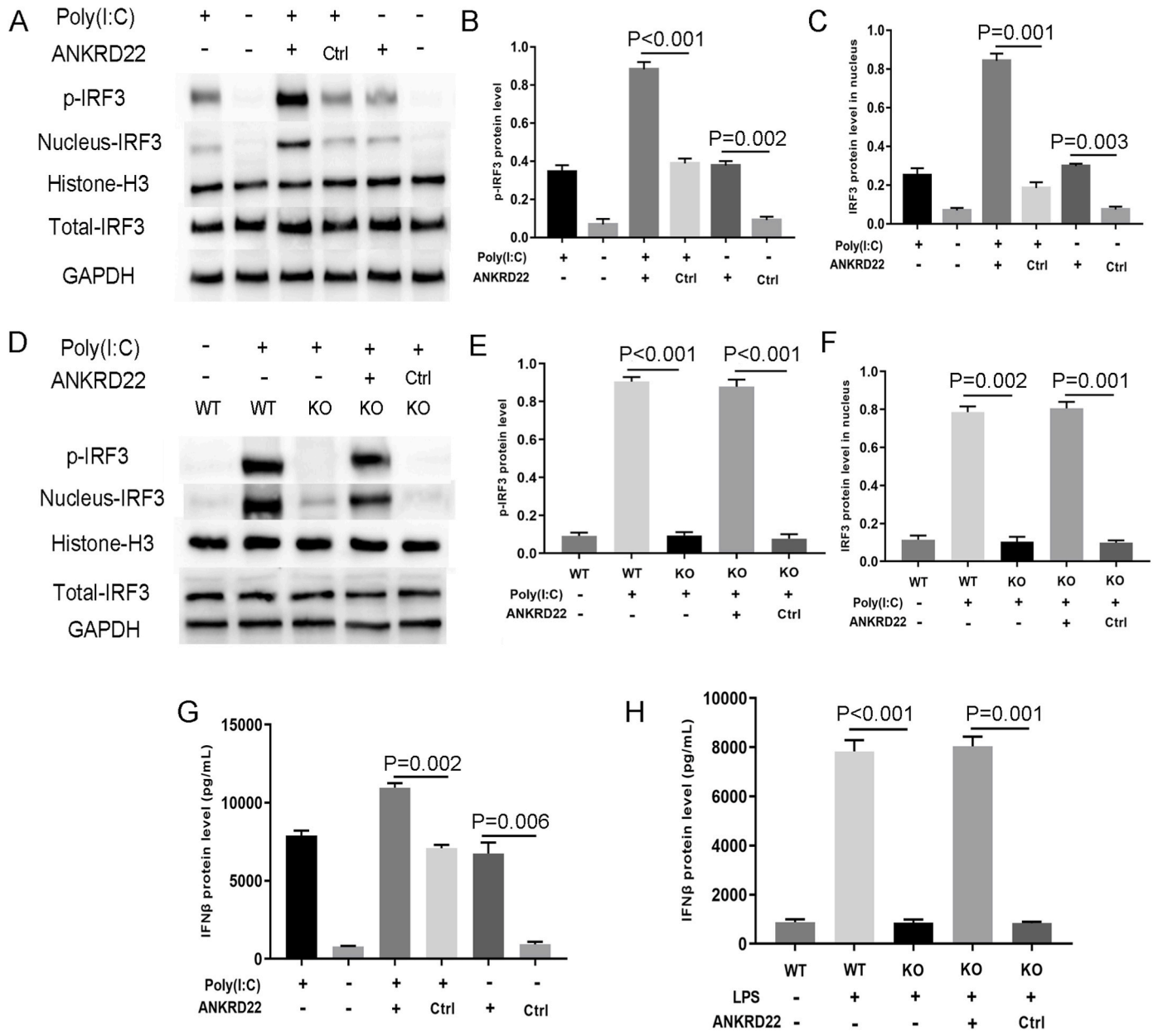

Fig. 5. ANKRD22 promotes macrophage M1 polarization by activating IRF3A-C. Effects of ANKRD22 overexpression on total IRF3, *p*-IRF3 and nuclear IRF3 protein expression in macrophages detected under different conditions by WB. D-F. Effects of ANKRD22 knockout on total IRF3, *p*-IRF3 and nuclear IRF3 protein expression in macrophages detected under different conditions by WB.G. The effect of ANKRD22 overexpression on the macrophage secretion levels of the proinflammatory cytokine IFN-β was evaluated by ELISA.H. The effect of ANKRD22 knockout on the macrophage secretion levels of the proinflammatory cytokine IFN-β was evaluated by ELISA. (n = 3, data are expressed as mean ± SD, each experiment was repeated three times).

overexpression group exhibited increased IFN-β secretion in macrophages, with or without the induction of poly (I:C).

Secretion of IFN-β was more pronounced in macrophages derived from wild-type mice after receiving poly (I:C) stimulation but was significantly reduced in the ANKRD22-KO group, which increased again after ANKRD22 expression was rescued (Fig. 5G–H). These results suggest that ANKRD22 regulates macrophage IRF3 activation as well as IFN-β secretion.

3.6. *ANKRD22 activates IRF3 by binding MAVS*

Fig. 5 demonstrates that the macrophage Rig-I receptor pathway is the downstream activation pathway of ANKRD22, and studies have proven that activation of IRF3 requires upstream MDA5 or RIG-I proteins to bind to MAVS proteins [31]. Our experimental results show coimmunoprecipitation between ANKRD22 and MAVS rather than with MDA5 (Fig. 6A). To determine whether ANKRD22 activates RIG-I by utilizing the classic MAVS pathway, we examined the effect of MAVS knockdown on RIG-I pathway protein expression. Compared with the sh-MAVS control group, the expression of iNOS, phosphorylation of IRF3 and nuclear expression of IRF3 in macrophages with high expression of ANKRD22 were significantly decreased (Fig. 6B–E). However, the expression of iNOS, phosphorylation of IRF3 and the level of nuclear IRF3 in macrophages with low expression of MAVS and high expression of ANKRD22 showed no significant changes compared with the ANKRD22 control group (Fig. 6B–E). These findings suggest that ANKRD22 requires MAVS to activate IRF3 to promote macrophage polarization (Fig. 7).

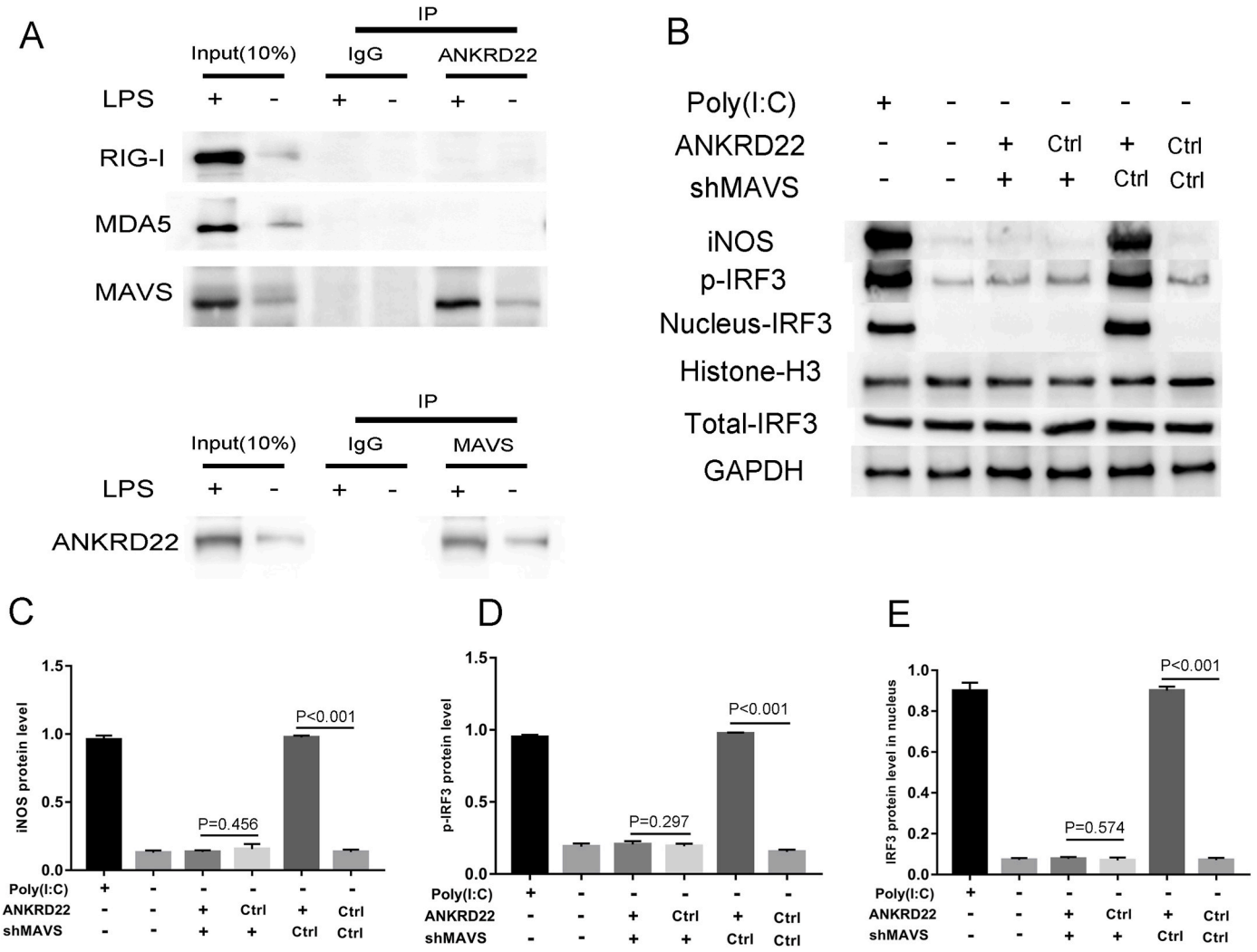

Fig. 6. ANKRD22 activates IRF3 by binding MAVS A. Immunoprecipitation to determine whether the binding of ANKRD22 to MAVS depends on the classical pathway (MDA5 or RIG-I). B. The effect of low MAVS expression on the expression of ANKRD22-activated IRF3 protein and iNOS was detected by WB. C. WB quantitative analysis of low MAVS expression inhibiting ANKRD22-enhanced iNOS protein expression levels. D. Low MAVS expression inhibited ANKRD22-enhanced *p*-IRF3 protein expression levels, as shown by WB quantitative analysis. E. Low MAVS expression inhibited ANKRD22-enhanced nuclear IRF3 protein expression levels, as shown by WB quantitative analysis (n = 3, data are expressed as mean ± SD, each experiment was repeated three times).

4. Discussion

Here, we found that ANKRD22 exacerbated sepsis-induced ARDS and promoted pulmonary macrophage M1 polarization. ANKRD22, a member of the ankyrin repeat motif (ANK) family, is an *N*-myristoylated protein mainly expressed in tumor cells, activated monocytes/macrophages, and epithelial cells [32, 33]. ANKRD22 could help repair damaged gastric mucosa by promoting the mobilization of $LGR5^{+}$ gastric epithelial cells via the upregulation of Wnt/β-catenin pathway activity in a mouse model [34]. Chen et al. found that low ANKRD22 levels in $CD11b^{+}HLA^{-}DR^{-}CD14^{-}CD15^{+}$ cells derived from primary ovarian tissues were associated with a more advanced stage and a higher recurrence rate. They identified ANKRD22 as a potential novel target for immunotherapy in ovarian cancer [35]. ANKRD22 up-regulated the transcription of E2F1, and promoted the progression of non-small cell lung cancer by enhancing cell proliferation. Therefore, regulating ANKRD2 expression can repair epithelial cell damage, maintain immune homeostasis and achieve disease treatment. In this study, we found that ANKRD22 expression was significantly elevated in the alveolar lavage fluid and blood of ARDS patients, as well as in the lung tissues of ARDS mice. Knockdown of ANKRD22 resulted in a significant reduction in lung injury scores and decreased in the secretion of pro-inflammatory factors in ARDS mice, suggesting that ANKRD22 is a critical molecule in exacerbating acute lung injury.

ANKRD22 is a critial molecule that regulates M1 polarization of pulmonary macrophage during ARDS. In recent years, ANKRD22 has been reported to be a novel metabolic reprogramming molecule involved in the occurrence of various tumors at different sites via various mechanisms [33, 34, 36–42]. However, few studies have investigated its role in the regulation of macrophage polarization. ANKRD22 expression was upregulated in activated macrophages in human kidney transplant biopsies [43] Liu Jet et al. found that ANKRD22 could promote the infiltration of inflammatory cells into damaged gastric tissue and increase mitochondrial Ca2+ influx and cytoplasmic nuclear factor production in macrophages [44]. This study found that elevated levels of ANKRD22 were associated with poor prognosis and M1 macrophage polarization in sepsis patients. In the septic ARDS model, ANKRD22 knockout mice also significantly reduced M1 polarization of lung macrophages. Up-regulation of ANKRD22 gene expression enhances M1 polarization in macrophages, whereas down-regulation attenuates M1 polarization in vitro. Therefore, ANKRD22 promotes the polarization of macrophage M1 during ARDS.

Activation of MAVS-IRF3 is critical for ANKRD22 to promote the polarization of macrophage M1. In the ANKRD22 downstream pathway,

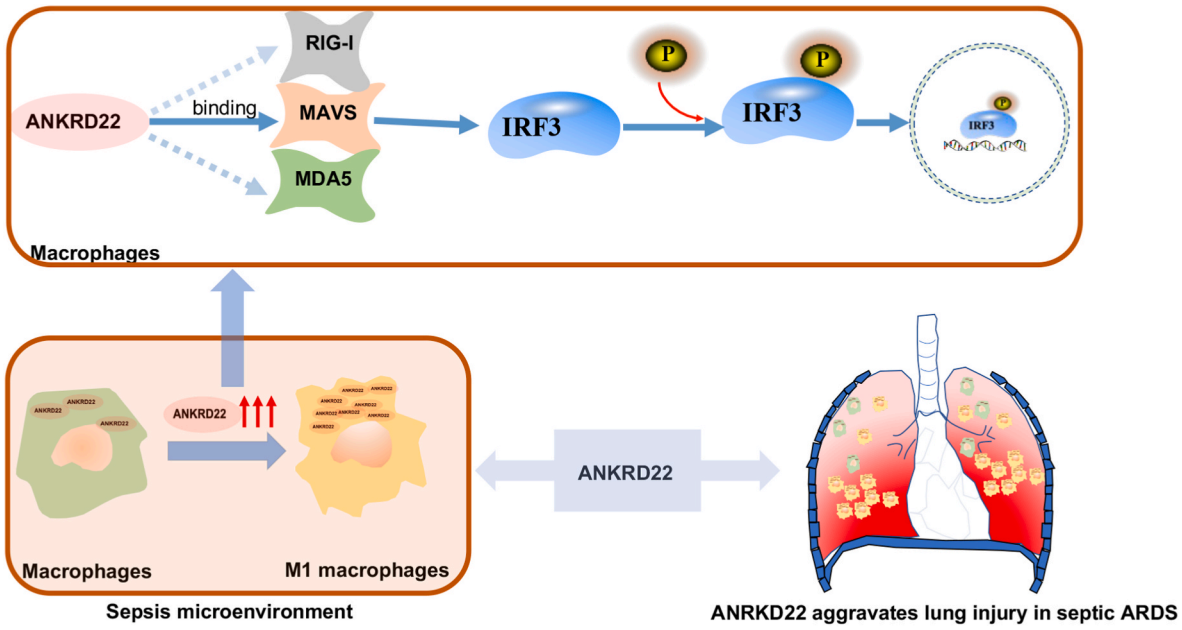

Fig. 7. ANRKD22 aggravates lung injury and promtes macrophage M1 polarization in septic ARDS.

RIG-I-like receptor pathway-related genes were significantly enriched when ANKRD22 expression was upregulated. Previous studies have reported that in response to viral infection, RIG-I-like RNA helicases bind to viral RNA and activate the mitochondrial protein MAVS, which in turn activating the transcription factors IRF3 and NF-κB to induce type I interferons [45] Poly I:C is recognized by the macrophage membrane helicase receptor RIG-I and the MDA5 molecule, leading to activation of the RLR pathway and subsequent activation of the MAVS-IRF3/7 cascade to produce effector molecules such as IFNβ and ISGs [46]. RIG-I and MDA-5 act together in the polarization of M1 macrophages in vivo, and they control infection by regulating the cellular polarization of target gene expression [47]. The mechanism may be that RIG-I and MDA-5 bind to the mitochondrial adaptor protein MAVS, which further forms a MAVS-IRF3 complex with IRF3 to initiate downstream signaling [48].

In this study, coimmunoprecipitation showed that LPS stimulation only enhanced the interaction of ANKRD22 with MAVS, but not with RIG-I or MDA5, and after MAVS knockdown in macrophages with high ANKRD22 expression, the expression levels of iNOS, phosphorylated IRF3 and nuclear IRF3 were significantly reduced. Previous studies have shown that the signaling domains (tetramer formation of RIG-I 2CARD) of RIG-I and MDA5 must form homo-oligomers to interact with MAVS to activate downstream signals [49], and this study shows that ANKRD22 acts directly on MAVS to activate IRF3 and promote the polarization of macrophage M1.

5. Conclusion

In summary, the present study suggests that ANKRD22 upregulation exacerbated sepsis-related ARDS. In this process, ANKRD22 may mediate IRF3 activation by binding to MAVS to promote macrophage M1 polarization. These findings indicate that targeted regulation of ANKRD22 may be an effective treatment for septic ARDS patients.

Funding

This study was supported by National Natural Science Foundation of China (grant numbers: 82202413), Natural Science Foundation of Shandong Province (grant numbers: ZR2022QH332), Scientific Research Start-up Funds for talent introduction of Jinan Central Hospital (grant numbers: YJRC2021010), Jinan Science and Technology Bureau's Clinical Technology Innovation Program (grant numbers: 202134058), Clinical Research cultivation Program of the Second Affiliated Hospital of Anhui Medical University (grant numbers: 2021LCYB12), Support Program for Elite Young Talents in Colleges and Universities of Anhui Province (grant numbers:gxyq2022006), National Natural Science Foundation Incubation Program of The Second Affiliated Hospital of Anhui Medical University (grant numbers: 2022GMFY10), and Natural Science Research Project of Anhui Higher Education Institutions (2023AH053168).

Availability of data and materials

Data supporting the results of this study are available from the corresponding author upon reasonable request.

Ethics approval and consent to participate

The study was conducted in accordance with the Declaration of Helsinki and approved by the Institutional Ethics Committee of the Affiliated Central Hospital of Shandong First Medical University (Ethics Committee Approval Number: JNCH2021-194-01) and the Animal Care and Use Committee of Jinan Central Hospital (Ethics Committee Approval Number: JNCH2021-114); and all human participants gave informed consent in writing.

Consent for publication

Written informed consent was obtained from all individuals.

CRediT authorship contribution statement

Shi Zhang: Conceptualization, Data curation, Writing - original draft, Writing - review & editing, Visualization, Resources, Validation. **Yao Liu:** Investigation, Methodology, Software. **Xiao-Long Zhang:** Investigation, Software. **Yun Sun:** Investigation, Methodology,

Software, Validation. **Zhong-Hua Lu:** Formal analysis, Methodology, Project administration, Resources, Supervision, Writing - original draft, Writing - review & editing.

Declaration of competing interest

The authors declare that they have no known competing financial interests or personal relationships that could have appeared to influence the work reported in this paper.

Data availability

Data will be made available on request.

Acknowledgements

Thanks to Dr. Wu Zong-sheng for his guidance on this article and AJE (part of Springer nature) for providing native language revisions to this article. Thanks to Dr. Guo Ping Chen for his contribution to this article on statistics.

Appendix A. Supplementary data

Supplementary data to this article can be found online at https://doi.org/10.1016/j.jtauto.2023.100228.

References

[1] G. Bellani, J.G. Laffey, T. Pham, et al., Epidemiology, patterns of care, and mortality for patients with acute respiratory distress syndrome in intensive care units in 50 countries, JAMA 315 (8) (2016) 788–800, https://doi.org/10.1001/jama.2016.0291.
[2] L. Liu, Y. Yang, Z. Gao, et al., Practice of diagnosis and management of acute respiratory distress syndrome in mainland China: a cross-sectional study, J. Thorac. Dis. 10 (9) (2018) 5394–5404, https://doi.org/10.21037/jtd.2018.08.137.
[3] C.L. Auriemma, H. Zhuo, K. Delucchi, et al., Acute respiratory distress syndrome-attributable mortality in critically ill patients with sepsis, Intensive Care Med. 46 (6) (2020) 1222–1231, https://doi.org/10.1007/s00134-020-06010-9.
[4] S. Lin, H. Wu, C. Wang, et al., Regulatory T cells and acute lung injury: cytokines, uncontrolled inflammation, and therapeutic implications, Front. Immunol. 9 (2018) 1545, https://doi.org/10.3389/fimmu.2018.01545.
[5] N.J. Meyer, L. Gattinoni, C.S. Calfee, Acute respiratory distress syndrome, Lancet (London, England) 398 (10300) (2021) 622–637, https://doi.org/10.1016/s0140-6736(21)00439-6.
[6] N.R. Aggarwal, L.S. King, F.R. D'Alessio, Diverse macrophage populations mediate acute lung inflammation and resolution, Am. J. Physiol. Lung Cell Mol. Physiol. 306 (8) (2014) L709–L725, https://doi.org/10.1152/ajplung.00341.2013.
[7] E.D. Morrell, P.K. Bhatraju, C.R. Mikacenic, et al., Alveolar macrophage transcriptional programs are associated with outcomes in acute respiratory distress syndrome, Am. J. Respir. Crit. Care Med. 200 (6) (2019) 732–741, https://doi.org/10.1164/rccm.201807-1381OC.
[8] Y.B. Chu, J. Li, P. Jia, et al., Irf1- and Egr1-activated transcription plays a key role in macrophage polarization: a multiomics sequencing study with partial validation, Int. Immunopharm. 99 (2021), 108072, https://doi.org/10.1016/j.intimp.2021.108072.
[9] S. Zhang, C. Chu, Z. Wu, et al., IFIH1 contributes to M1 macrophage polarization in ARDS, Front. Immunol. 11 (2020), 580838, https://doi.org/10.3389/fimmu.2020.580838.
[10] B. Guillen-Guio, J.M. Lorenzo-Salazar, S.F. Ma, et al., Sepsis-associated acute respiratory distress syndrome in individuals of European ancestry: a genome-wide association study, Lancet Respir. Med. 8 (3) (2020) 258–266, https://doi.org/10.1016/s2213-2600(19)30368-6.
[11] L. Barrot, P. Asfar, F. Mauny, et al., Liberal or conservative oxygen therapy for acute respiratory distress syndrome, N. Engl. J. Med. 382 (11) (2020) 999–1008, https://doi.org/10.1056/NEJMoa1916431.
[12] Z. Lu, S. Meng, W. Chang, et al., Mesenchymal stem cells activate Notch signaling to induce regulatory dendritic cells in LPS-induced acute lung injury, J. Transl. Med. 18 (1) (2020) 241, https://doi.org/10.1186/s12967-020-02410-z.
[13] J. Liu, P.S. Zhang, Q. Yu, et al., Losartan inhibits conventional dendritic cell maturation and Th1 and Th17 polarization responses: Novel mechanisms of preventive effects on lipopolysaccharide-induced acute lung injury, Int. J. Mol. Med. 29 (2) (2012) 269–276, https://doi.org/10.3892/ijmm.2011.818.
[14] S. Hu, J. Li, X. Xu, et al., The hepatocyte growth factor-expressing character is required for mesenchymal stem cells to protect the lung injured by lipopolysaccharide in vivo, Stem Cell Res. Ther. 7 (1) (2016) 66, https://doi.org/10.1186/s13287-016-0320-5.
[15] C.C. Dos Santos, H. Amatullah, C.M. Vaswani, et al., Mesenchymal stromal (stem) cell therapy modulates miR-193b-5p expression to attenuate sepsis-induced acute lung injury, Eur. Respir. J. 59 (1) (2022), https://doi.org/10.1183/13993003.04216-2020.
[16] S. Pal, P. Nath, S. Biswas, et al., Nonylphenol attenuates SOCS3 expression and M1 polarization in lipopolysaccharide-treated rat splenic macrophages, Ecotoxicol. Environ. Saf. 174 (2019) 574–583, https://doi.org/10.1016/j.ecoenv.2019.03.012.
[17] J. Zou, T. Kawai, T. Tsuchida, et al., Poly IC triggers a cathepsin D- and IPS-1-dependent pathway to enhance cytokine production and mediate dendritic cell necroptosis, Immunity 38 (4) (2013) 717–728, https://doi.org/10.1016/j.immuni.2012.12.007.
[18] C. Anfray, F. Mainini, E. Digifico, et al., Intratumoral combination therapy with poly(I:C) and resiquimod synergistically triggers tumor-associated macrophages for effective systemic antitumoral immunity, J. Immunother. Cancer 9 (9) (2021), https://doi.org/10.1136/jitc-2021-002408.
[19] Y. Xi, J. Shi, W. Li, et al., Histone modification profiling in breast cancer cell lines highlights commonalities and differences among subtypes, BMC Genom. 19 (1) (2018) 150, https://doi.org/10.1186/s12864-018-4533-0.
[20] C.A. Meyer, X.S. Liu, Identifying and mitigating bias in next-generation sequencing methods for chromatin biology, Nat. Rev. Genet. 15 (11) (2014) 709–721, https://doi.org/10.1038/nrg3788.
[21] Y. Wang, K. Wang, J. Fu, HDAC6 mediates macrophage iNOS expression and excessive nitric oxide production in the blood during endotoxemia, Front. Immunol. 11 (2020) 1893, https://doi.org/10.3389/fimmu.2020.01893.
[22] T.N. Golden, A. Venosa, A.J. Gow, Cell origin and iNOS function are critical to macrophage activation following acute lung injury, Front. Pharmacol. 12 (2021), 761496, https://doi.org/10.3389/fphar.2021.761496.
[23] T. Liu, M. Feng, Z. Wen, et al., Comparison of the characteristics of cytokine storm and immune response induced by SARS-CoV, MERS-CoV, and SARS-CoV-2 infections, J. Inflamm. Res. 14 (2021) 5475–5487, https://doi.org/10.2147/jir.S329697.
[24] L. Wang, H. Zhang, L. Sun, et al., Manipulation of macrophage polarization by peptide-coated gold nanoparticles and its protective effects on acute lung injury, J. Nanobiotechnol. 18 (1) (2020) 38, https://doi.org/10.1186/s12951-020-00593-7.
[25] F. Liu, J. Xie, X. Zhang, et al., Overexpressing TGF-β1 in mesenchymal stem cells attenuates organ dysfunction during CLP-induced septic mice by reducing macrophage-driven inflammation, Stem Cell Res. Ther. 11 (1) (2020) 378, https://doi.org/10.1186/s13287-020-01894-2.
[26] E. Nistal-Villán, E. Rodríguez-García, M. Di Scala, et al., A RIG-I 2CARD-mavs200 chimeric protein reconstitutes IFN-β induction and antiviral response in models deficient in type I IFN response, J. Innate Immun. 7 (5) (2015) 466–481, https://doi.org/10.1159/000375262.
[27] L. Zhang, W. Li, Y. Sun, et al., Activation of activating Fc gamma receptors down-regulates the levels of interferon β, interferon γ and interferon λ1 in porcine alveolar macrophages during PRRSV infection, Int. Immunopharm. 81 (2020), 106268, https://doi.org/10.1016/j.intimp.2020.106268.
[28] Y. Ren, F.A. Khan, N.S. Pandupuspitasari, et al., Highly pathogenic porcine reproductive and respiratory syndrome virus modulates interferon-β expression mainly through attenuating interferon-regulatory factor 3 phosphorylation, DNA Cell Biol. 35 (9) (2016) 489–497, https://doi.org/10.1089/dna.2016.3283.
[29] Y. Song, H. Dou, W. Gong, et al., Bis-N-norgliovictin, a small-molecule compound from marine fungus, inhibits LPS-induced inflammation in macrophages and improves survival in sepsis, Eur. J. Pharmacol. 705 (1–3) (2013) 49–60, https://doi.org/10.1016/j.ejphar.2013.02.008.
[30] Y. Song, X. Liu, H. Yue, et al., Anti-inflammatory effects of benzenediamine derivate FC-98 on sepsis injury in mice via suppression of JNK, NF-κB and IRF3 signaling pathways, Mol. Immunol. 67 (2 Pt B) (2015) 183–192, https://doi.org/10.1016/j.molimm.2015.05.005.
[31] D. Arnoult, F. Soares, I. Tattoli, et al., An N-terminal addressing sequence targets NLRX1 to the mitochondrial matrix, J. Cell Sci. 122 (Pt 17) (2009) 3161–3168, https://doi.org/10.1242/jcs.051193.
[32] T. Utsumi, T. Hosokawa, M. Shichita, et al., ANKRD22 is an N-myristoylated hairpin-like monotopic membrane protein specifically localized to lipid droplets, Sci. Rep. 11 (1) (2021), 19233, https://doi.org/10.1038/s41598-021-98486-8.
[33] T. Pan, J. Liu, S. Xu, et al., ANKRD22, a novel tumor microenvironment-induced mitochondrial protein promotes metabolic reprogramming of colorectal cancer cells, Theranostics 10 (2) (2020) 516–536, https://doi.org/10.7150/thno.37472.
[34] R. Wang, Y. Wu, Y. Zhu, et al., ANKRD22 is a novel therapeutic target for gastric mucosal injury, Biomed. Pharmacother. 147 (2022), 112649, https://doi.org/10.1016/j.biopha.2022.112649.
[35] H. Chen, K. Yang, L. Pang, et al., ANKRD22 is a potential novel target for reversing the immunosuppressive effects of PMN-MDSCs in ovarian cancer, J. Immunother. Cancer (2) (2023) 11, https://doi.org/10.1136/jitc-2022-005527.
[36] C.S. Yang, K.Y. Chang, T.M. Rana, Genome-wide functional analysis reveals factors needed at the transition steps of induced reprogramming, Cell Rep. 8 (2) (2014) 327–337, https://doi.org/10.1016/j.celrep.2014.07.002.
[37] J. Yin, W. Fu, L. Dai, et al., ANKRD22 promotes progression of non-small cell lung cancer through transcriptional up-regulation of E2F1, Sci. Rep. 7 (1) (2017) 4430, https://doi.org/10.1038/s41598-017-04818-y.
[38] Y. Wu, H. Liu, Y. Gong, et al., ANKRD22 enhances breast cancer cell malignancy by activating the Wnt/β-catenin pathway via modulating NuSAP1 expression, Bosn. J. Basic Med. Sci. 21 (3) (2021) 294–304, https://doi.org/10.17305/bjbms.2020.4701.

[39] M.L. Wissing, S.G. Kristensen, C.Y. Andersen, et al., Identification of new ovulation-related genes in humans by comparing the transcriptome of granulosa cells before and after ovulation triggering in the same controlled ovarian stimulation cycle, Hum. Reprod. (Oxf.) 29 (5) (2014) 997–1010, https://doi.org/10.1093/humrep/deu008.

[40] M.L. Grøndahl, C.Y. Andersen, J. Bogstad, et al., Specific genes are selectively expressed between cumulus and granulosa cells from individual human pre-ovulatory follicles, Mol. Hum. Reprod. 18 (12) (2012) 572–584, https://doi.org/10.1093/molehr/gas035.

[41] M. Wu, X. Li, T. Zhang, et al., Identification of a nine-gene signature and establishment of a prognostic nomogram predicting overall survival of pancreatic cancer, Front. Oncol. 9 (2019) 996, https://doi.org/10.3389/fonc.2019.00996.

[42] L. Luo, Y. Li, C. Huang, et al., A new 7-gene survival score assay for pancreatic cancer patient prognosis prediction, Am. J. Cancer Res. 11 (2) (2021) 495–512.

[43] J.M. Venner, K.S. Famulski, D. Badr, et al., Molecular landscape of T cell-mediated rejection in human kidney transplants: prominence of CTLA4 and PD ligands, Am. J. Transplant. : Off. J. Am. Soc. Transplantation Am. Soc. Transplant Surgeons 14 (11) (2014) 2565–2576, https://doi.org/10.1111/ajt.12946.

[44] J. Liu, J. Wu, R. Wang, et al., ANKRD22 drives rapid proliferation of Lgr5(+) cells and acts as a promising therapeutic target in gastric mucosal injury, Cellular and Molecular Gastroenterol. Hepatol. 12 (4) (2021) 1433–1455, https://doi.org/10.1016/j.jcmgh.2021.06.020.

[45] F. Hou, L. Sun, H. Zheng, et al., MAVS forms functional prion-like aggregates to activate and propagate antiviral innate immune response, Cell 146 (3) (2011) 448–461, https://doi.org/10.1016/j.cell.2011.06.041.

[46] A. Vats, D. Gautam, J. Maharana, et al., Poly I:C stimulation in-vitro as a marker for an antiviral response in different cell types generated from Buffalo (Bubalus bubalis), Mol. Immunol. 121 (2020) 136–143, https://doi.org/10.1016/j.molimm.2020.03.004.

[47] A.E.L. Stone, R. Green, C. Wilkins, et al., RIG-I-like receptors direct inflammatory macrophage polarization against West Nile virus infection, Nat. Commun. 10 (1) (2019) 3649, https://doi.org/10.1038/s41467-019-11250-5.

[48] S. Liu, X. Cai, J. Wu, et al., Phosphorylation of innate immune adaptor proteins MAVS, STING, and TRIF induces IRF3 activation, Science (New York, N.Y.) 347 (6227) (2015) aaa2630, https://doi.org/10.1126/science.aaa2630.

[49] B. Wu, S. Hur, How RIG-I like receptors activate MAVS, Current opinion in virology 12 (2015) 91–98, https://doi.org/10.1016/j.coviro.2015.04.004.